The effect of wheel rotation on the rolling noise predictions

Christopher Knuth[1], Giacomo Squicciarini[1] and David Thompson[1]

[1] Institute of Sound and Vibration Research, University of Southampton, SO17 1BJ, UK
C.Knuth@soton.ac.uk

Abstract. The effect of the wheel rotation on its sound radiation in rolling noise predictions is investigated. The wheel response is modelled using a finite element model that can account for the different effects introduced by rotation and together with TWINS the radiated sound power is determined. Noise and vibration data are compared over a range of typical train speeds, between a stationary wheel, a rotating wheel where rotation is replaced by a moving load, and a rotating wheel that also includes the inertial forces. Compared with the most complete model, differences in the wheel sound power level of up to 6 dB in one-third octave bands are found if the stationary wheel is used instead. The differences remain below 2 dB for speeds up to 500 km/h if the rotation is approximated with a moving load. In terms of the total A-weighted sound power level of the wheel, the stationary wheel underestimates the noise by up to 3 dB, while the differences are less than 1 dB for a moving load. Generally, the differences introduced by the approximate representations of the wheel rotation are smaller than the uncertainties that are inevitable in rolling noise predictions. The results show that in rolling noise predictions for usual train speeds the wheel rotation is sufficiently well approximated by a moving load, which is the method implemented in TWINS.

Keywords: Rolling noise, wheel rotation, moving load, sound radiation.

1 Introduction

Rolling noise is one of the most important sources of noise in railways and is caused by the excitation of the wheel and the track from their combined surface roughness [1]. One of the most commonly used rolling noise prediction models is TWINS [2,3], which requires models of the wheel and track vibration, their noise radiation and the roughness as an input.

For modelling the wheel vibration, finite element models are commonly used that treat it as a stationary structure, which is an incomplete representation in case of a moving train. The classic approach to account for the wheel rotation that is used in TWINS is to replace the rotation with a moving load, that rotates around the wheel circumference at the same angular velocity [4]. This causes the wheel modes to be split into two co- and counter-rotating waves that, when viewed from the excitation point, are shifted in frequency by $\pm n\Omega/2\pi$, where n is the number of nodal diameters and Ω the angular velocity. However, this approach neglects the gyroscopic and centrifugal effects.

In recent years, finite element models that include the inertial forces in the equation of motion of a rotating structure have been developed [5,6,7]. The kinematics can be defined in a non-rotating (Eulerian) or rotating (Lagrangian) frame of reference. For the interaction of the rolling wheel with the track, the non-rotating frame is preferred.

Baeza et al. [5,6] used Eulerian coordinates to establish an equation of motion of the rotating wheelset directly in a non-rotating reference frame that can be solved with the finite element method. Sheng et al. [7] developed a model in which the kinematics of the rotating wheelset were defined in a rotating frame and converted the response to the non-rotating frame by applying a transformation. This was implemented using axisymmetric finite elements. The moving load is an attractive simplification of the effect of wheel rotation, but according to [7,8], a fully rotating model should be implemented for correct modelling of rolling noise at high train speeds.

In this work, the effect of the wheel rotation on the prediction of the radiated sound power of rolling noise is investigated to quantify the differences caused by the various modelling approximations for a wide range of train speeds.

2 Methodology

2.1 Model of the rotating railway wheel

In this study, an axisymmetric finite element model that adopts the Eulerian approach of Baeza et al. [5,6] has been implemented for modelling the rotating railway wheelset. Additionally, a geometric stiffness matrix can be included, as proposed in [9]. For more information, the reader is referred to the references. The model has been validated against a 3D model of a rotating wheel in the commercial software COMSOL Multiphysics. The equation of motion (EOM) of the rotating structure can be written as

$$\mathbf{M}\ddot{\mathbf{u}} + (2\Omega\mathbf{G} + \mathbf{D})\dot{\mathbf{u}} + \big(\mathbf{K} + \Omega^2(\mathbf{K}_g - \mathbf{C})\big)\mathbf{u} = \Omega^2\mathbf{f}_c + \mathbf{f} \tag{1}$$

where $\mathbf{M}$ is the mass, $\mathbf{D}$ the damping, and $\mathbf{K}$ the stiffness matrix of the stationary wheel, $\mathbf{u}$ is the displacement vector and $\mathbf{f}$ is the force vector. The additional terms are due to the rotation at angular velocity Ω and can be described as follows. The matrix $\mathbf{G}$ accounts for the gyroscopic effects due to the inertial Coriolis forces. Matrix $\mathbf{C}$ contains terms that alter the stiffness of the structure, such as spin softening due to the inertial centrifugal force. In the non-rotating frame, a frequency shift of $\pm n\Omega/2\pi$ is added to the rotating waves by the definition of $\mathbf{G}$ and $\mathbf{C}$. The geometric stiffness matrix $\mathbf{K}_g$ adds stress-stiffening in the presence of the constant centrifugal force $\mathbf{f}_c$. Although $\mathbf{f}_c$ is included on the right-hand side, it does not contribute to harmonic vibration at an angular frequency ω and is only non-zero for $n = 0$ nodal diameters.

In the axisymmetric model, the displacements are written as a Fourier series of spatial harmonics n in the circumferential direction θ as

$$\mathbf{u}(r, z, \theta) = \sum_{n=-\infty}^{\infty} \mathbf{u}_n(\mathrm{r}, \mathrm{z}) e^{\mathrm{i}n\theta}, \tag{2}$$

which allows the EOM to be solved for each harmonic separately. The solutions consist of co- and counter rotating waves (for $n \neq 0$).

2.2 Modelling the sound radiation of the wheel

The wheel model is coupled with TWINS to calculate its radiated sound power. An analytical track model of a UIC60 rail with continuous support is adopted [1]. The vertical pad stiffness is 250 MN/m per rail with a loss factor of 0.2 and the half sleeper is modelled as a rigid mass of 140 kg supported by a ballast stiffness of 200 MN/m with a loss factor of 1.0. These values are converted to equivalent continuous ones using a sleeper spacing of 0.6 m. The wheel-track interaction and the wheel response are obtained in a non-rotating frame. The roughness spectrum is based on the ISO 3095:2013 limit curve [10]. To determine the overall wheel sound power, the spatially averaged wheel velocities for each nodal diameter (combination of the harmonics $-n$ and $+n$) are combined with the approximate wheel radiation efficiencies from [11]. Mobilities from different wheel models are used to investigate the importance of including the rotation. They correspond to a stationary wheel, and rotating wheels in which the rotation is either replaced by a moving load or fully accounted for by the Eulerian approach.

3 Results

3.1 Effect of the rotation on the wheel modes and frequency response

To illustrate the effect of wheel rotation, the frequency response is considered first. For this, a wheel with a straight web and radius of 0.43 m is adopted, see **Fig. 1**. It is constrained at the hub to replace the axle and the rigid body motion of the full wheelset is added separately. Three different cases are shown: a stationary wheel, a rotating wheel, in which the rotation is replaced by a moving load [4], and the rotating wheel based on the Eulerian approach including the inertial forces. The driving point mobilities are compared in **Fig. 1** for a radial force and train speed of 300 km/h, i.e. $\Omega = 194$ rad/s or 31 Hz. When the wheel rotation is included, resonances with $n \neq 0$ split into two peaks with a reduced height compared with the stationary case. With the moving load, the frequency split is exactly $\pm n\Omega/2\pi$ for all modes. The split is different for some resonances in the Eulerian model due to the gyroscopic and centrifugal effects, see for example the peaks around 2.1 kHz. The phenomena are explained in more detail below.

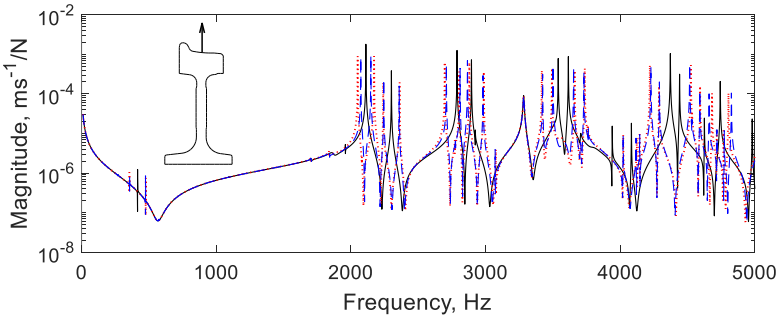

Fig. 1. Driving point mobility of the wheel for radial excitation and a velocity of 300 km/h; —, stationary wheel; · · ·, rotating wheel (moving load); – – –, rotating wheel (Eulerian model).

The impact of the gyroscopic and centrifugal effects on the split of the natural frequencies, if observed in the non-rotating reference frame, is illustrated in **Fig. 2** for the nodal diameters $n = 1$ and $n = 2$. The gyroscopic effect splits the frequencies of the two modes in proportion to Ω. Thus, the rotating waves can no longer form a standing wave, as in the stationary wheel. Axial modes are well approximated by the moving load with $\pm n\Omega/2\pi$, as they barely generate Coriolis forces. The Coriolis acceleration, determined by the cross product of the angular velocity vector with the velocity vector $2(0,0,\Omega)^T \times (\dot{u},\dot{v},\dot{w})^T = 2\Omega(-\dot{v},\dot{u},0)^T$, is zero for the axial $\dot{w}$, but non-zero for the radial $\dot{u}$ and circumferential $\dot{v}$ velocity components. The frequency shift of a radial mode can be reduced by up to $\pm\Omega/2\pi$ when compared with the moving load if it generates considerable Coriolis forces. Since modes have coupled radial/axial motion, the Coriolis shift is neither zero nor reaches $\mp\Omega/2\pi$. Consequently, the overall frequency shift is between $\pm(n-1)\Omega/2\pi$ and $\pm n\Omega/2\pi$ for radial modes. Circumferential modes are increased in frequency compared with the moving load, due to the different direction of the Coriolis force. Thus, the frequency shift of circumferential modes lies between $\pm n\Omega/2\pi$ and $\pm(n+1)\Omega/2\pi$. For larger n, the same trends can be observed.

Additionally, the centrifugal effect shifts both modes equally towards higher (stress-stiffening), or lower (spin softening) frequencies, in proportion to Ω^2. Stress-stiffening is larger for axial modes, as it increases the bending stiffness of the web. The centrifugal effects are small compared with the gyroscopic effects at usual train speeds [7].

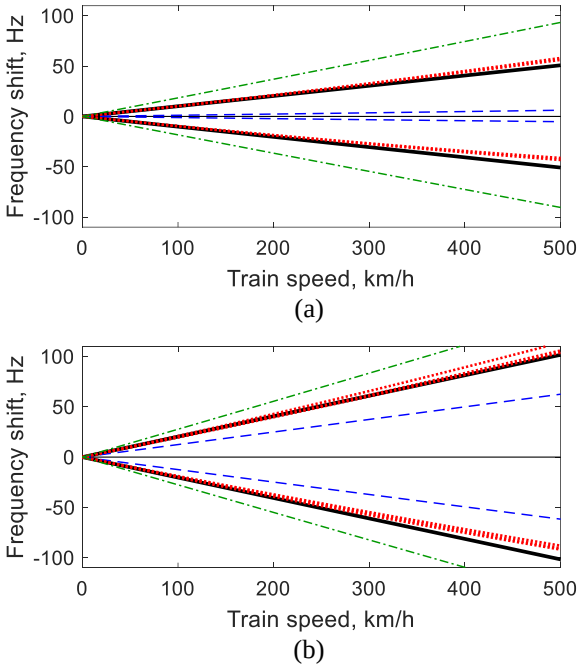

Fig. 2. Frequency shift of the wheel modes in the non-rotating frame of reference for the nodal diameters (a) $n = 1$ (b) $n = 2$; —, stationary wheel; ▬, rotating wheel (moving load); – – –, rotating radial modes (Eulerian model); · · ·, rotating axial modes (Eulerian model); – · –, rotating circumferential modes (Eulerian model).

3.2 Radiated sound power of the rotating wheel

The sound power radiated by the wheel has been calculated for train speeds from 10 to 500 km/h in steps of 10 km/h. The sound power level (SWL) of an example wheel with a straight web is shown in **Fig. 3** in one-third octave bands for a roughness input that is based on the ISO 3095 limit curve [10] with suitable contact filter. Spectra are shown for speeds of 80, 160 and 250 km/h, together with 500 km/h ($\Omega = 323$ rad/s) to see the continuing trend at higher speeds. Results are shown for the stationary wheel, the rotating wheel using the moving load approximation and the Eulerian model without the stress-stiffening term. As expected, the sound power increases with increasing speed.

Below 400 Hz, the three models agree well. Above this frequency, there are differences of up to 6 dB between the stationary wheel and the rotating models, especially in the region below 2 kHz, where the wheel has fewer resonances. The differences increase as the train speed increases. Above 2 kHz, the difference reduces to about 3 dB. In most frequency bands the stationary wheel underestimates the noise compared with the two rotating wheel models. The differences between the Eulerian model and the moving load approximation remain much smaller than 1 dB at the lower speeds, but at 500 km/h they can be as high as 2 dB in some bands.

The stationary wheel response consists of standing waves, as the rotating waves with harmonics $\pm n$ coincide in frequency and combine coherently. Consequently, the wheel response, calculated as the spatially averaged velocity over the wheel circumference, is smaller than the rotating case. In the rotating case the responses of the harmonics $+n$ and $-n$ are calculated separately and added incoherently, as the two waves have their resonance at different frequencies.

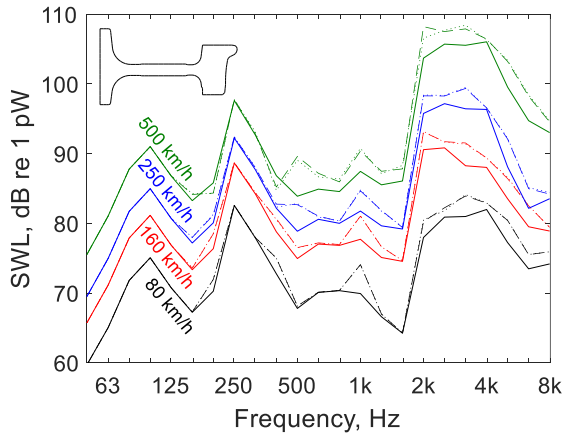

Fig. 3. Sound power level of the wheel for train speeds of 80, 160, 250 and 500 km/h with ISO 3095 roughness; —, stationary wheel; · · ·, rotating wheel (moving load); – – –, rotating wheel (Eulerian model).

The total A-weighted SWL of the wheel can be calculated from these spectra and is found to increase with the train speed V by approximately $30 \log_{10} V$ between 50 and 500 km/h. The differences in these total A-weighted SWL of the wheel relative to those

for the Eulerian model are plotted against train speed in **Fig. 4**. As well as the wheel with a straight web considered above, results are also shown for a wheel with a curved web with a radius of 0.42 m. If the stationary wheel model is used, the total SWL is underestimated by up to 3 dB, compared with the Eulerian model, which agrees with [8]. At very low speeds (<40 km/h), the difference is around 1-2 dB. Above 100 km/h, the stationary model gives slightly better agreement for the wheel with straight web.

If the rotation is approximated with a moving load, the differences remain much smaller than 1 dB for all the train speeds considered. Above 400 km/h the moving load shows an increase up to around 0.6 dB for the wheel with the curved web, which is not seen for the wheel with a straight web. Results are also shown for variants of the Eulerian model: one that includes the additional geometric stress-stiffening, which was omitted in the previous results, another without the Coriolis force and a third without the inertial centrifugal force. Adding stress-stiffening or suppressing the centrifugal force changes the total SWL by less than 0.2 dB for the two tested wheels. Excluding the Coriolis force has a similar effect to using the moving load, since the remaining centrifugal terms in the equation of motion are negligible.

The results have also been calculated using a measured roughness spectrum, but are not shown here. While the SWL spectra were different from those in **Fig. 3**, the relative differences in total SWL were found to be very similar to the ones shown in **Fig. 4**.

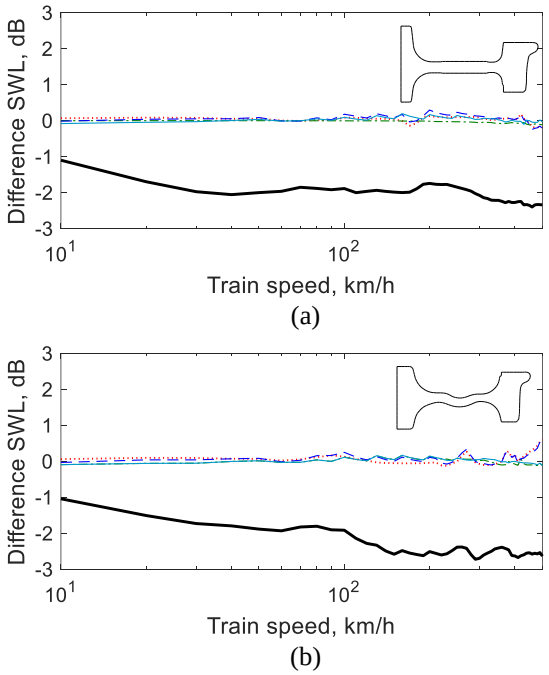

Fig. 4. Difference of total A-weighted wheel sound power level between the Eulerian model and rotation approximations with increasing train speed of a wheel with (a) straight web and (b) curved web; ▬, stationary wheel; · · ·, rotating wheel (moving load); – – –, Eulerian without Coriolis force; —, Eulerian without centrifugal force; – · –, Eulerian with stress-stiffening.

3.3 Comparison of the response in a non-rotating and rotating frame

In TWINS the wheel response, and consequently its sound radiation, is calculated in a rotating frame of reference. The rotating frame was preferred in TWINS to allow comparisons with measured data from accelerometers fixed to the rotating wheel [4]. In the present work, a non-rotating frame is used, which seems more appropriate for noise calculations.

Fig. 5(a) shows the mean square velocity averaged around the circumferential direction for the straight-webbed wheel at a speed of 300 km/h. Results are given for the axial direction at the middle of the web and the radial direction at the contact point. In **Fig. 5**(b) the differences in the total A-weighted SWL of the wheel are shown against speed. When calculating the wheel response in a rotating frame with the moving load, the resonance peaks in the response are no longer split [4]. Hence, the one-third octave band results differ from those in the non-rotating frame. The spectral differences in the velocity can be as high as 8 dB, but are generally lower, especially at frequencies above 2 kHz, which are most important for the wheel contribution to the noise. The trends are similar for other speeds and similar relative differences occur in the SWL spectra. The overall A-weighted SWL differs by less than 0.5 dB if the rotating rather than the non-rotating frame is used to calculate the noise radiated from the wheel. The level difference is again smaller than the uncertainty in rolling noise predictions.

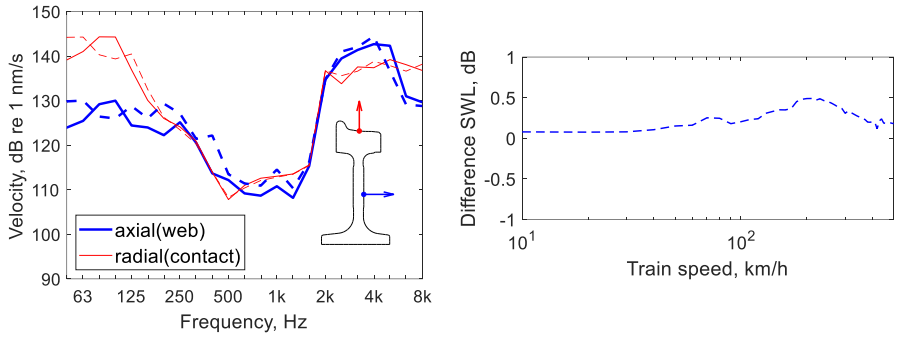

(a) (b)

Fig. 5. Comparison of results obtained in a different frame of reference (a) velocity at web and contact position for a wheel at 300 km/h and (b) difference in total A-weighted SWL of the wheel; —, non-rotating frame; – – –, rotating frame.

4 Conclusions

The effect of the rotation of a railway wheel on its sound radiation has been investigated using numerical wheel models that represent the rotation with different levels of approximation combined with the TWINS model. Three wheel models were implemented: (i) a stationary wheel, (ii) a rotating wheel in which the rotation is replaced by a moving load, and (iii) a rotating wheel that also includes the inertial forces and geometric stiffening effects.

Spectral differences of up to 6 dB are found in the SWL spectra when not fully accounting for the rotation. The overall A-weighted SWL is underestimated by up to 3 dB if the rotation is completely neglected. If the rotation is represented by a moving load the differences in SWL are smaller than 1 dB. The impact of the inertial forces on the overall SWL is marginal and in all cases much less than 1 dB. Hence, the moving load model is a sufficient representation of the rotation at normal train speeds. The impact of the inertial forces cannot be easily generalized, as the additional change of the resonances depends on the speed of the wheel and its geometry. The differences found when approximating the rotation with a moving load are smaller than the uncertainty of rolling noise predictions [3], e.g. due to the variability of measured roughness [12]. If the wheel response is calculated in a rotating, rather than a non-rotating frame of reference, similar differences are found. Altogether, the study has shown that the approximations made in the TWINS model [2-4] have only a marginal effect on the noise predicted from the wheel even at very high speeds.

References

1. Thompson, D.J.: Railway Noise and Vibration: Mechanisms, Modelling and Means of Control. 1st edn. Elsevier, Amsterdam (2009).
2. Thompson, D.J., Hemsworth, B., Vincent, N.: Experimental validation of the TWINS prediction program for rolling noise, part 1: description of the model and method. Journal of Sound and Vibration 193(1), 123-135 (1996).
3. Thompson, D.J., Fodiman, P., Mahé, H.: Experimental validation of the TWINS prediction program for rolling noise, part 2: results. Journal of Sound and Vibration 193(1), 137-147 (1996).
4. Thompson, D.J.: Wheel rail noise generation, part V: Inclusion of wheel rotation. Journal of Sound and Vibration 161(3), 467-482 (1993).
5. Baeza, L., Giner-Navarro, J., Thompson, D.J., Monterde, J.: Eulerian models of the rotating flexible wheelset for high frequency railway dynamics. Journal of Sound and Vibration 449, 300-314 (2019).
6. Baeza, L., Giner-Navarro, J., Thompson, D.J.: Reply to “Discussion on ‘Eulerian models of the rotating flexible wheelset for high frequency railway dynamics’ [J. Sound Vib. 449 (2019) 300-314]”. Journal of Sound and Vibration 489, 115665 (2020).
7. Sheng, X., Liu, Y.X., Zhou, X.: The response of a high-speed train wheel to a harmonic wheel-rail force. Journal of Physics: Conference Series 744, 012145 (2016).
8. Cheng, G., He, Y., Han, J., Sheng, X., Thompson, D.J.: An investigation into the effects of modelling assumptions on sound power radiated from a high-speed train wheelset. Journal of Sound and Vibration 495, 115910 (2021).
9. Genta, G.: Dynamics of Rotating Systems. 1st edn. Springer, New York (2005).
10. ISO 3095:2013 Acoustics — Railway applications — Measurement of noise emitted by railbound vehicles
11. Thompson, D.J., Jones, C.J.C.: Sound radiation from a vibrating railway wheel. Journal of Sound and Vibration 253(2), 401-419 (2002).
12. Squicciarini, G., Toward, M.G.R., Thompson, D.J., Jones, C.J.C.: Statistical Description of Wheel Roughness. In: Nielsen, J., et al. (eds), Noise and Vibration Mitigation for Rail Transportation Systems. Notes on Numerical Fluid Mechanics and Multidisciplinary Design, vol 126. Springer, Berlin, Heidelberg (2015).